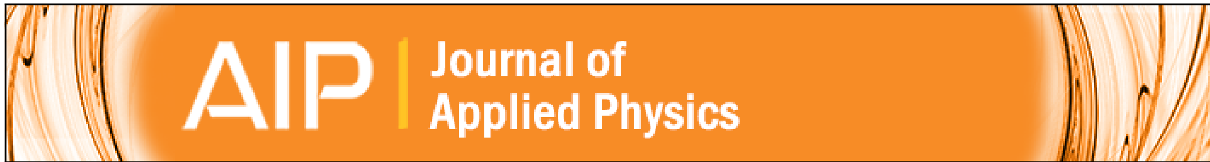

Characterization of Ba Ti 1 x Zr x O 3 thin films obtained by a soft chemical spin-coating technique

F. M. Pontes, M. T. Escote, C. C. Escudeiro, E. R. Leite, E. Longo, A. J. Chiquito, P. S. Pizani, and J. A. Varela

Citation: Journal of Applied Physics **96**, 4386 (2004); doi: 10.1063/1.1775048
View online: http://dx.doi.org/10.1063/1.1775048
View Table of Contents: http://scitation.aip.org/content/aip/journal/jap/96/8?ver=pdfcov
Published by the AIP Publishing

Re-register for Table of Content Alerts

Create a profile.

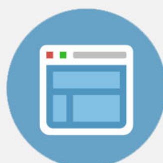

Sign up today!

[This article is copyrighted as indicated in the article. Reuse of AIP content is subject to the terms at: http://scitation.aip.org/termsconditions. Downloaded to] IP: 186.217.234.225 On: Tue, 14 Jan 2014 13:05:48

HTML ABSTRACT + LINKS

Characterization of $BaTi_{1-x}Zr_xO_3$ thin films obtained by a soft chemical spin-coating technique

F. M. Pontes, M. T. Escote, C. C. Escudeiro, E. R. Leite, and E. Longo[a)]
LIEC, CMDMC, Department of Chemistry, UFSCar, Via Washington Luiz, km 235, CP-676, CEP-13565-905, São Carlos, S. P., Brazil

A. J. Chiquito and P. S. Pizani
Department of Physics, UFSCar-Via Washington Luiz, km 235, CEP-13565-905, São Carlos, S. P., Brazil

J. A. Varela
Institute of Chemistry, UNESP, Araraquara, S. P., Brazil

(Received 15 September 2003; accepted 30 May 2004)

Single-phase perovskite structure $BaZr_xTi_{1-x}O_3$ (BZT) $(0.05 \leqslant x \leqslant 0.25)$ thin films were deposited on Pt–Ti–SiO_2–Si substrates by the spin-coating technique. The structural modifications in the thin films were studied using x-ray diffraction and micro-Raman scattering techniques. Lattice parameters calculated from x-ray data indicate an increase in lattice (a axis) with the increasing content of zirconium in these films. Such Zr substitution also result in variations of the phonon mode wave numbers, especially those of lower wave numbers, for $BaZr_xTi_{1-x}O_3$ thin films, corroborate to the structural change caused by the zirconium doping. On the other hand, Raman modes persist above structural phase transition, although all optical modes should be Raman inactive in the cubic phase. The origin of these modes must be interpreted as a function of a local breakdown of the cubic symmetry, which could be a result of some kind of disorder. The BZT thin films exhibited a satisfactory dielectric constant close to 181–138, and low dielectric loss tan $\delta < 0.03$ at the frequency of 1 kHz. The leakage current density of the BZT thin films was studied at elevated temperatures and the data obey the Schottky emission model. Through this analysis the Schottky barrier height values 0.68, 1.39, and 1.24 eV were estimated to the BZT5, BZT15, and BZT25 thin films, respectively. © *2004 American Institute of Physics*. [DOI: 10.1063/1.1775048]

I. INTRODUCTION

The development of thin film technology has been receiving great investments due to the possibility of achieving a greater miniaturization of integrated electronic circuits used nowadays. Barium titanate ($BaTiO_3$) is one of the most studied perovskite-type materials, especially due to its potentiality applications such as capacitive and nonvolatile memory cells (DRAMs and FRAMs), electro-optical integrated circuits, pyroelectric devices, etc.[1–3] It is well known that homovalent and heterovalent substitutions of barium or titanium ions give rise to various behaviors including relaxor properties, which may appear for some composition-temperature ranges.[4–6] Additions such as strontium are employed to lower the Curie temperature T_c, which decreases linearly with the increase of the strontium content. Recently, it was reported that the ferroelectric phase transition in $Ba_{0.8}Sr_{0.2}TiO_3$ thin films occurs near room temperature.[7] In a similar way, the substitution of Zr ions on Ti sites changes strongly the character of the dielectric response close to Curie temperature of $BaTi_{1-x}Zr_xO_3$ bulk ceramics and thin films.[8,9] When the Zr content is higher (>27%), the $BaTi_{1-x}Zr_xO_3$ ceramics exhibit typical relaxor-like behavior, in which the T_c raises with the increase in frequency.[10] In this sense, studies have been performed for the preparation of $BaTi_{1-x}Zr_xO_3$ thin films by different techniques and their structural, microstructural and electrical characteristics have been studied.[11–13]

Dixit *et al.*[6] reported the phase transition behavior of sol gel derived $BaZr_{0.4}Ti_{0.6}O_3$ thin films and a relaxor-type behavior was observed in such compounds. Pantou *et al.*[9] studied thin films of the solid solution $BaTi_{1-x}Zr_xO_3$ prepared by MOCVD (metal organic chemical vapor deposition) technique and with x varying from 0.00 to 0.80. Meanwhile, for higher Zr concentration $(x > 0.25)$ a secondary ZrO_2 phase was detected by x-ray diffraction.

In this work, $BaTi_{1-x}Zr_xO_3$ thin films $(0.05 \leqslant x \leqslant 0.25)$ were prepared by a soft chemical method and deposited by the spin-coating technique.[14–16] X-ray diffraction, micro-Raman, atomic force microscopy were used to characterize the structural and microestructural evolution of the thin films. Dielectric measurements at different Zr contents were also performed on the films at room temperature. We have also investigated the current conduction mechanism based on the interface limited Schottky emission theory and estimated the possible physical parameters involved.

II. EXPERIMENT

The BZT, or more precisely $BaTi_{1-x}Zr_xO_3$, thin films studied in the present work were derived from a soft chemical processing with Zr contents ranging from 0.05 to 0.25.

[a)]Author to whom correspondence should be addressed. Telephone: +55-16-260-8214; Fax: +55-16-260-8350. Electronic mail address: liec@power.ufscar.br

 © 2004 American Institute of Physics

[This article is copyrighted as indicated in the article. Reuse of AIP content is subject to the terms at: http://scitation.aip.org/termsconditions. Downloaded to] IP: 186.217.234.225 On: Tue, 14 Jan 2014 13:05:48

The precursor materials were barium carbonate ($BaCO_3$), titanium (IV) isopropoxide ($Ti(OCH(CH_3)_3)_4$), zirconium-tetra-n-butoxide ($Zr(OC_4H_9)_4$). Deionized water, citric acid, and ethylene glycol were used as solvents or complexing agents. Titanium citrate and zirconium citrate were formed by the dissolution of, respectively, titanium (IV) isopropoxide and zirconium-tetra-n-butoxide in water solutions of citric acid, under constant agitation. After homogenization of the solutions containing Ti and Zr, they were mixed in the molar proportions of 5:95, 15:85, and 25:75 of zirconium and titanium, respectively. The citrate solution was well stirred for some hours at 60 °C to yield a clear and homogenous solution. After homogenization the $BaCO_3$ was slowly added, while stirring vigorously. After homogenization of this solution, ethylene glycol was added to promote mixed citrate polymerization by the polyesterification reaction. With continued heating at 80–90 °C, the solution became more viscous, albeit devoid of any visible phase separation. The viscosity of the deposition solution was adjusted to 20 mPas by controlling the water content. The polymeric solution was spin-coated on the substrates by a commercial spinner operating at 7000 rev/min for 30 s (spin-coater KW-4B, Chemat Technology). In the case, such solution was deposited onto the substrates via a syringe filter to avoid particulate contamination. The substrate used was $Pt-Ti-SiO_2-Si$. After the depositions, the films were kept in ambient air at 150 °C on a hot plate for 20 min to remove residual solvents. The heat treatment was carried out in two stages: initial heating at 400 °C for 4 h at a heating rate of 5 °C/min to pyrolyze the organic materials, followed soon thereafter by heating at 700 °C for 2 h to crystallize the films.

The film thickness was controlled by adjusting the number of coatings and each layer was oxidized at 400 °C and crystallized at 700 °C before the next coating of the layer. These coating–drying operations were repeated until the desired thickness was obtained.

The BZT thin films were structurally characterized by x-ray diffraction (XRD) (Cu K_α radiation) in the mode of $\theta - 2\theta$ scan, recorded on a Rigaku diffractometer.

The morphology and grain size were studied by atomic force microscopy (AFM). These images were taken using a Digital Instruments Multimode Nanoscope IIIa. The micro-Raman measurements were performed at room temperature as a function of the Zr content, using the 514.5 nm line of an argon ion laser as the excitation source. The power was kept at 15 mW and a 100× lens was used. The spectra were recorded using a T-64 Jobin-Yvon triple-monochromator coupled to a CCD detector. The film thickness was evaluated observing the cross-section of the films using a Zeiss DSM940A scanning electron microscopy (SEM).

The dielectric properties were measured in the films in a metal-thin film-metal configuration, using a HP4192A impedance/gain phase analyzer. To measure electrical properties, Au dot electrodes of 4.90×10^{-2} mm^2 area were deposited by evaporation process on the surfaces of the heat-treated films as top electrodes, through a shadow mask. In order to achieve a contact with the platinum bottom electrode, a corner of the film was etched away using a HF +HCl mixed solution. All the measurements were conducted at room temperature.

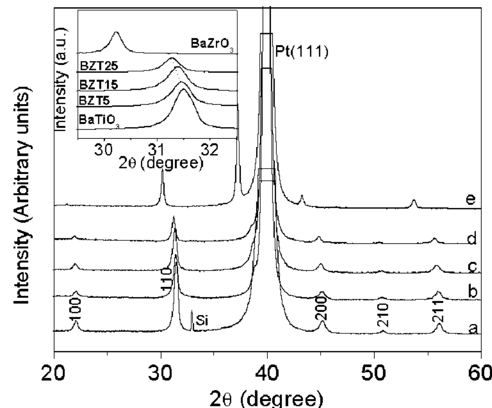

FIG. 1. X-ray diffraction patterns of $BaZr_xTi_{1-x}O_3$ thin films as a function of the Zr (x) content. (a) $x=0$, (b) $x=0.05$, (c) $x=0.15$, (d) $x=0.25$, and (e) $x=1$. The inset shows selected 2θ region of the (110) diffraction peak.

III. RESULTS AND DISCUSSION

The x-ray diffraction patterns of the $BaTi_{1-x}Zr_xO_3$ thin films with different Zr contents ($x=0.05$, 0.15, and 0.25) annealed at 700 °C are shown in Fig. 1. These samples will be herein after called as BZT5, BZT15, and BZT25. The diffraction patterns of the pure $BaTiO_3$ and $BaZrO_3$ thin films are also presented for comparison. The x-ray patterns indicate that the samples are polycrystalline and single phase. However, in the BZT thin films, they were prepared by MOCVD and displaying a higher Zr content, a ZrO_2 secondary phase was found.[9] The polycrystalline nature in these thin films is due to a lattice mismatch between BZT and the $Pt-Ti-SiO_2-Si$ substrate. All the diffraction peaks, except the strong peak at $2\theta\sim39°$ belonging to the Pt substrates, are characteristic of the perovskite structure. The inset in Fig. 1 shows the (110) diffraction peaks of BZT thin films. It is clear that with the increase of the Zr content the peaks shift to lower diffraction angles. This indicates an increase in the lattice parameter caused by the fact that the electronic density of Zr ions is higher than the electronic density of Ti ions and, therefore, the substitution of Ti by Zr ions leads to an expansion in the unit cell. Through these data, we verify that the BZT5 sample crystallize in an orthorhombic structure, although the BZT15 and BZT25 thin films seems to crystallize in cubic structure. Meanwhile, Dobal *et al.* suggested that BZT15 compounds presents a rombohedral structure.[8] In order make sure of the symmetry in which the film BZT15 crystallize, we have analyzed the XRD pattern by means of the Rietveld method using the FULLPROF program. It is important to notice that it is a qualitative analyze and we have assumed the structural models corresponding to the appropriate space group symmetry: (a) Pm3m for cubic system, and (b) Amm2 for the orthorhombic one, as reported for the $BaTiO_3$ compound in the literature.[17] Also for this analyze we have excluded the 2θ region between $35<2\theta<44°$, that correspond to the more intense Bragg reflection of the Pt on bottom of the substrate. In fact, through this analysis, we

[This article is copyrighted as indicated in the article. Reuse of AIP content is subject to the terms at: http://scitation.aip.org/termsconditions. Downloaded to] IP: 186.217.234.225 On: Tue, 14 Jan 2014 13:05:48

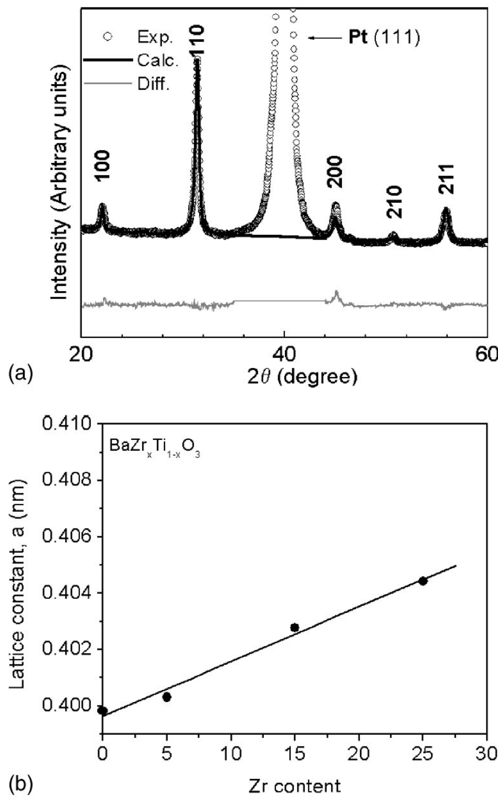

FIG. 2. (a) Calculated (full line) and experimental (open circle) x-ray diffraction patterns of the BZT15 thin film. The bottom line is the difference between the experimental and calculated x-ray diffractograms; (b) evolution of the lattice parameter as a function of the Zr composition in $BaZr_xTi_{1-x}O_3$ thin films.

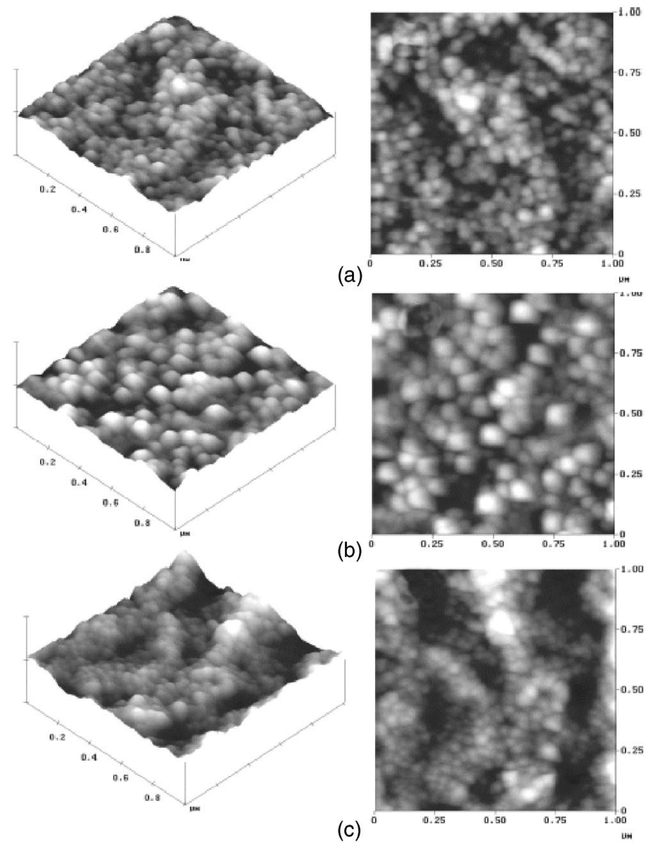

FIG. 4. Surface microstructure of the $BaZr_xTi_{1-x}O_3$ thin films with different compositions obtained by atomic force microscopy: (a) $x=0.05$, (b) $x=0.15$ and (c) $x=0.25$.

found that the BZT $x=0.015$ seems to crystallize in a cubic structure, as shown in Fig. 2. We believe that such difference could be attributed to the mismatch between the interface film/substrate. The lattice constants of the BZT thin films were determined from these refined XRD patterns, as shown in Fig. 2(b). In addition, the evolution from the tetragonal to the cubic structures of the BZT thin films is further confirmed by a micro-Raman scattering study.

The room temperature Raman spectra of BZT thin films are compared with the pure $BaTiO_3$ thin film spectrum in Fig. 3. Through this figure, we verify the evolution of the

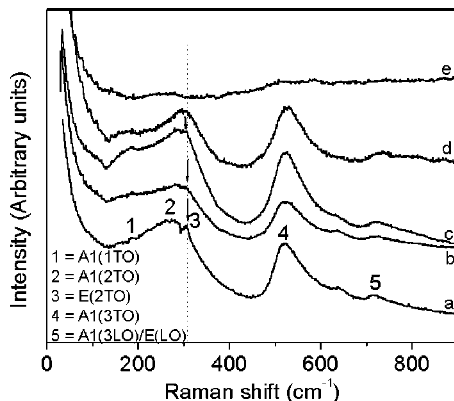

FIG. 3. Raman spectra of $BaZr_xTi_{1-x}O_3$ thin films at room temperature with different compositions: (a) $x=0$, (b) $x=0.05$, (c) $x=0.15$, (d) $x=0.25$ and (e) $x=1$.

Raman spectra with Zr substitution on the BZT thin films. It is important to notice that a similar behavior was observed in Raman spectra of BZT compounds reported in literature.[8] The $BaTiO_3$ spectra revealed the presence of a tetragonal structure, mainly characterized by the $A_1(1TO)$, $A_1(2TO)$, E(2TO), $A_1(3TO)$, and $A_1(3LO)/E(LO)$ Raman modes. For such compound, the E(2TO) ($\sim 307\ cm^{-1}$) phonon mode indicates an asymmetry within the TiO_6 octahedra, which suggest the presence of a tetragonal crystalline structure.[18] This figure also revealed that the E(2TO) mode become weaker with the increase of the Zr content. Such behavior indicate that the substitution of Ti by Zr in the $BaTiO_3$ structure results in structural disorder and, consequently, in structural phase transition. In the spectra pf BZT15 and BZT25, we can observe three factors: (a) A similar spectra as that reported for a cubic BZT ($x=0.2$) compounds;[8] (b) the absence of $A_1(1TO)$ mode; and (c) a new Raman mode at $\sim 150\ cm^{-1}$. In agreement with the x-ray results, these results suggest a possible cubic crystalline structure for the BZT15 and BZT25 films.

Meanwhile, the disorders caused by the Zr substitution destroy the perfect cubic local symmetry and thus allows Raman activity in the cubic phase. It is important to notice that the conversion point for the structural phase transition could occur for Zr concentration $x<0.15$, but more work is needed to a precise determination of such conversion point.

The evolution of the microstructure of BZT thin films, as a function of Zr content is shown in Fig. 4. Through an

[This article is copyrighted as indicated in the article. Reuse of AIP content is subject to the terms at: http://scitation.aip.org/termsconditions. Downloaded to] IP: 186.217.234.225 On: Tue, 14 Jan 2014 13:05:48

TABLE I. The root-mean-square (rms) surface roughness and average grain size of the BZT thin films evaluated from atomic force microscopy.

Parameters	BZT5	BZT15	BZT25
Grain size (nm)	60	90	40
Roughness (nm)	4.0	4.5	3.7

analysis of these AFM images, we have observed that the average grain size was significantly enhanced with the increase of the Zr content in the range 0.05–0.15. In addition, overall observations of thin films indicate a good microstructure with no discontinuities in terms of pinholes and microcracks. On the other hand, with the increase of Zr content for concentration higher than 0.15 the same morphology is still observed and thus become dense, smoother and with smaller grain size. Dixit *et al.*[19] observed similar behavior in a wide Zr doping level for the Zr-doped $BaTiO_3$ thin films prepared by sol-gel technique. Table I lists the root-mean-square surface roughness and average grain size of the BZT thin films evaluated from the atomic force microscopy results.

The dielectric properties of the BZT thin films in an Au/BZT/Pt configuration were measured at room temperature as a function of the applied frequency. Figure 5 shows the clear evolution of the dielectric constant for the films with $0.05 < x \leqslant 0.15$. It can be seen that the value of the dielectric constant increases, while it decreases with a further increase in the Zr content for $x = 0.25$. This behavior could be addressed to the following effects: (1) The increasing of the Zr content $(0.05 \leqslant x \leqslant 0.15)$ results in higher the grain size values, and such effect increases the dielectric constant; (2) for Zr content $x \geqslant 0.25$, we observed a decrease in grain size of the film, and it moves the ferroelectric to paraelectric phase transition temperature to ~298 K,[20] such combination of effects reduces the dielectric constant at room temperature. This behavior is in good agreement with previous results by AFM measurements. Wu *et al.*[21] also observed similar behavior for BZT thin films prepared by rf magnetron sputtering, where the value of the dielectric constant decreased in the following order: BZT12 > BZT22 > BZT40. In addition, recent investigation by Pantou *et al.*[9] on the behavior of the dielectric properties in BZT thin films prepared by MOCVD verified the following order for the values of the

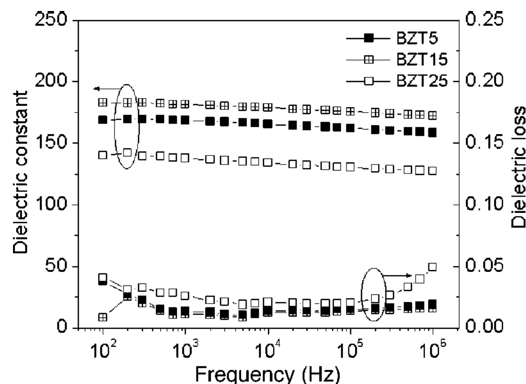

FIG. 5. Room temperature dielectric constant and dielectric loss (tan δ) of $BaZr_xTi_{1-x}O_3$ thin films with different Zr compositions as a function of the measuring frequency.

TABLE II. Dielectric constant of BZT thin films, herein obtained and according to the literature at the frequency of 1 kHz.

Reference	BZT5	BZT10	BZT15	BZT20	BZT25
9	145		170		130
21		100			
26				150	
This work	168		181		138

dielectric constants: BZT15 > BZT25 ⩾ BZT5 > BZT30. Table II shows the dielectric constants of thin films herein measured at room temperature compared with other BZT thin films reported elsewhere.

In order to study the current transport mechanism in BZT thin films, the current-voltage characteristics curves were obtained at different diode temperatures and the results are plotted in Fig. 6. The metal–BZT–metal system usually

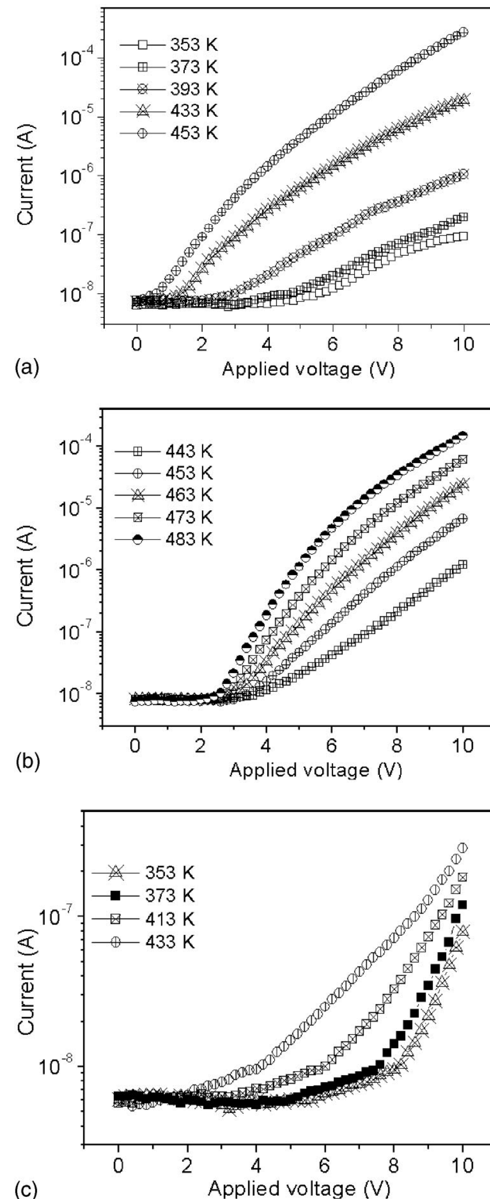

FIG. 6. The characteristics of the positive I–V curves obtained at different temperatures for the BZT thin films studied in this work.

[This article is copyrighted as indicated in the article. Reuse of AIP content is subject to the terms at: http://scitation.aip.org/termsconditions. Downloaded to] IP: 186.217.234.225 On: Tue, 14 Jan 2014 13:05:48

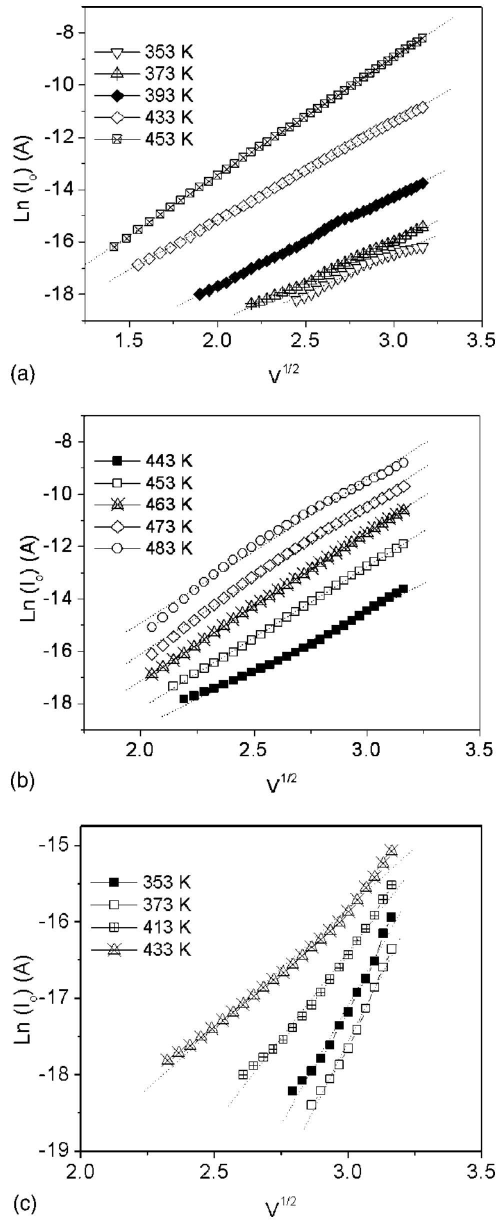

FIG. 7. Variation of $\ln(I_o)$ as a function of $V^{1/2}$ for the BZT thin films at different temperature.

constitutes a back-to-back Schottky diode. The current density in such system is given by

$$J = \left[A * T^2 \exp\left(\frac{-q(\phi_B - \Delta\phi_B)}{kT} \right) \right] \left[\exp\left(\frac{qV}{nkT} \right) - 1 \right], \quad (1)$$

where V is the applied voltage, T is the temperature, n is the ideality factor, ϕ_B is the Schottky barrier height, and A^* ($=120$ m/m$_0$, m$_0$ is the free hole mass) is the Richardson constant.

As expected from the Schottky current emission theory, the current increases by increasing temperature, because this thermally activated conduction is further enhanced by the applied field. We also have investigated the use of the Poole–Frenkel and space-charge-limited current models, but the fit of the experimental data using these models was quite unreasonable. Figure 7 shows the relation of $\ln(I_o)$ versus $V^{1/2}$ for

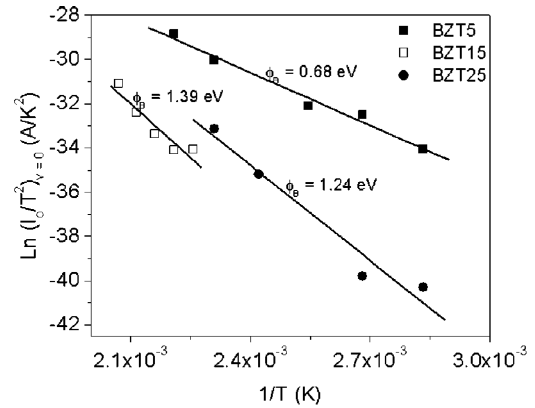

FIG. 8. Plot of $\ln(I_o/T^2)$ vs $1/T$ for BZT thin films, in which the Schottky barrier height was estimated.

the high current emission measured at different temperatures. The logarithm of current [ln (I_o)] was found to be linearly dependent of the square root of applied voltage in the interest region, suggesting that the Schottky emission occurs. In this sense, in Fig. 8 we plotted the $\ln(I_0/T^2)_{v=0}$ versus $1/T$ curves, for the different BZT compositions, (high field region). From these curves we evaluated the barrier heights from the slopes of the plots $\ln(I_0/T^2)_{v=0}$ versus $1/T$. In fact, the barrier height (at $V=0$) reflects the Schottky barrier heights of 0.68, 1.39, and 1.24 eV for BZT5, BZT15, and BZT25 thin films, respectively, considering the thermionic emission only. Wu and Shy reported that the current emission of the BZT12 thin films deposited on $LaNiO_3$ followed the relation of Schottky emission and a Schottky barrier height of 0.73 eV was evaluated from the temperature dependence of the current emission.[13] In addition, Scott *et al.* reported values of the Schottky barrier (at $V=0$) for $SrBiTa_2O_9$ (SBT), $Ba_{1-x}Sr_xTiO_3$ (BST) and $PbZr_{0.4}Ti_{0.6}O_3$ (PZT) to be about 1.6, 1.62, and 1.5 eV, respectively.[22] Also, Das *et al.* studied the leakage characteristics of $SrBi_2Ta_2O_6$ thin films at elevated temperatures and the data were fitted by the Schottky emission model.[23] The Schottky barrier heights of the films on Pt and $LaNiO_3$ substrates were estimated to be 1.27 and 1.12 eV, respectively. Other authors have reported the Schottky barrier height of the $SrBi_2Nb_2O_9$ and (Ba,Sr)TiO_3 thin films in the range of 1.37–1.5 eV.[24,25]

IV. CONCLUSIONS

We have produced polycrystalline $BaZr_xTi_{1-x}O_3$ thin films with different Zr contents, by a soft solution process. Raman spectra and x-ray diffraction analyses carried out in the $BaZr_xTi_{1-x}O_3$ thin films showed that the Zr addition results in a structural phase transitions, that depend on the Zr content. In fact, we verify that the BZT5 crystallize in an orthorhombic structure, while the BZT15 and BZT25 display a cubic structure. AFM analyses showed that the surface roughness and the grain size of $BaZr_xTi_{1-x}O_3$ thin films decrease as the Zr concentration increases up to 0.15. All these thin films had a homogenous and dense microstructure with a smooth surface.

The electrical measurements of the capacitors with BZT thin films revealed dielectric constant at 1 kHz varying from

[This article is copyrighted as indicated in the article. Reuse of AIP content is subject to the terms at: http://scitation.aip.org/termsconditions. Downloaded to] IP: 186.217.234.225 On: Tue, 14 Jan 2014 13:05:48

168 to 181 when the Zr content was increased from 0.05 to 0.15, but such the value dropped to 138 when $x = 0.25$, which could be attributed to a smaller grain size. In addition, all the BZT thin films exhibited a low dielectric loss of tan $\delta < 0.03$. The leakage current data are in agreement with the Schottky emission model and the Schottky barrier height was estimated to be 0.68, 1.39, and 1.24 eV for the BZT5, BZT15, and BZT25 thin films, respectively.

These results indicated that the physical properties of the BZT thin films displayed a strong dependence on the content of Zr.

ACKNOWLEDGMENTS

The authors gratefully acknowledge the financial support of the Brazilian financing agencies FAPESP/CEPID, CNPq/PRONEX, and CAPES.

[1] M. C. Wang, F. Y. Hsiao, C. S. Hsi, and N. C. Wu, J. Cryst. Growth **246**, 78 (2002).
[2] E. K. Evangelou, N. Konofaos, and C. B. Thomas, Philos. Mag. B **80**, 395 (2000).
[3] P. U. Sastry, Pramana, J. Phys. **59**, 547 (2002).
[4] R. Maier and J. L. Cohn, J. Appl. Phys. **92**, 5429 (2002).
[5] R. Farhi, M. El Marssi, A. Simon, and J. Ravez, Eur. Phys. J. B **18**, 605 (2000).
[6] A. Dixit, S. B. Majumder, R. S. Katiyar, A. S. Bhalla, Appl. Phys. Lett. **82**, 2679 (2003).
[7] F. M. Pontes, E. R. Leite, D. S. L. Pontes, E. Longo, E. M. S. Santos, S. Mergulhão, P. S. Pizani, F. Lanciotti, T. M. Boschi, and J. A. Varela, J. Appl. Phys. **91**, 5972 (2002).
[8] P. S. Dobal, A. Dixit, R. S. Katiyar, Z. Yu, R. Guo, and A. S. Bhalla, J. Appl. Phys. **89**, 8085 (2001).
[9] R. Pantou, C. Dubourdieu, F. Weiss, J. Kreisel, G. Köbernik, and W. Haessler, Mater. Sci. Semicond. Process. **5**, 237 (2003).
[10] Z. Yu, C. Ang, R. Guo, and A. S. Bhalla, J. Appl. Phys. **92**, 2655 (2002).
[11] C. S. His, C. Y. Chen, N. C. Wu, and M. C. Wang, J. Appl. Phys. **94**, 598 (2003).
[12] W. S. Choi, J. H. Boo, J. Yi, and B. Hong, Mater. Sci. Semicond. Process. **5**, 211 (2003).
[13] T. B. Wu and H. J. Shy, Ceram. Int. **26**, 599 (2000).
[14] F. M. Pontes, C. D. Pinheiro, E. Longo, E. R. Leite, S. R. de Lazaro, J. A. Varela, P. S. Pizani, T. M. Boschi, and F. Lanciotti, Mater. Chem. Phys. **78**, 227 (2002).
[15] F. M. Pontes, S. H. Leal, P. S. Pizani, M. R. M. C. Santos, E. R. Leite, E. Longo, F. Lanciotti, T. M. Boschi, and J. A. Varela, J. Mater. Res. **18**, 659 (2003).
[16] N. S. L. S. Vasconcelos, J. S. Vasconcelos, V. Bouquet, S. M. Zanetti, E. R. Leite, E. Longo, L. E. B. Soledade, F. M. Pontes, M. Guilloux-Viry, A. Perrin, M. I. Bernardi, and J. A. Varela, Thin Solid Films **436**, 213 (2003).
[17] G. H. Kwel, A. C. Lawson, S. J. L. Billinge, and S.-W. Cheong, J. Phys. Chem. **97**, 2368 (1993).
[18] S. Gupta, J. Raman Spectrosc. **33**, 42 (2002).
[19] A. Dixit, S. B. Majumder, A. Savvinov, R. S. Katiyar, R. Guo, and A. S. Bhalla, Mater. Lett. **56**, 933 (2002).
[20] D. Hennings, A. Schnell, and G. Simon, J. Am. Ceram. Soc. **65**, 539 (1982).
[21] T. B. Wu, C. M. Wu, and M. L. Chen, Appl. Phys. Lett. **69**, 2659 (1996).
[22] J. F. Scott, K. Watanabe, A. J. Hartmann, and R. N. Lamb, Ferroelectrics **225**, 83 (1999).
[23] R. R. Das, P. Bhattacharya, R. S. Katiyar, and A. S. Bhalla, J. Appl. Phys. **92**, 6160 (2002).
[24] R. R. Das, P. Bhattacharya, W. Perez, R. S. Katiyar, and A. S. Bhalla, Appl. Phys. Lett. **81**, 880 (2002).
[25] J. F. Scott, Jpn. J. Appl. Phys., Part 1 **38**, 2277 (1999).
[26] N. Kamehara, M. Tsukada, J. S. Cross, and K. Kurihara, J. Am. Ceram. Soc. **105**, 801 (1997).

[This article is copyrighted as indicated in the article. Reuse of AIP content is subject to the terms at: http://scitation.aip.org/termsconditions. Downloaded to] IP: 186.217.234.225 On: Tue, 14 Jan 2014 13:05:48